Journal of Materials Chemistry C

ROYAL SOCIETY OF CHEMISTRY

PAPER

View Article Online
View Journal | View Issue

Cite this: J. Mater. Chem. C, 2025, 13, 18305

Aggregation induced emission *versus* aggregation caused quenching: tuning the emission behaviour of liquid crystalline materials†

Thorben Neumann,[a] Sidharth Thulaseedharen Nair Sailaja,[a] Jens Voskuhl[a] and Michael Giese*[ab]

Received 16th May 2025,
Accepted 30th June 2025

DOI: 10.1039/d5tc01954k

rsc.li/materials-c

Luminescent liquid crystals have attracted attention over the past decades. In this study we introduce a new concept for thermo-responsive luminescent materials. The unique combination of two classes of luminophores, showing either aggregation-induced emission (AIE) or aggregation-caused quenching (ACQ) within a liquid crystalline matrix, yielded an emission shift from green (534 nm) to red (619 nm). Thereby, the emission color is controlled by the state of aggregation within the liquid crystalline material, which can be controlled by temperature. This temperature-controlled material mimics an emissive traffic light and is suitable as a thermo sensor warning of heat.

Introduction

Emissive liquid crystalline (LC) materials represent a combination of responsive mesomorphic structures with the ability to emit light. Therefore, they are promising for the development of *e.g.* optoelectronics (organic light emitting diodes, display technology, *etc.*), data storage and sensing applications.[1–6] A common challenge in the design of emissive LC materials is aggregation caused quenching (ACQ). This phenomenon is observed due to strong π–π-interactions in ordered phases like the mesophase and the crystalline state. In this context, luminophores exhibiting aggregation induced emission (AIE) have gained tremendous interest.[7–9] The increased order in the LC-phase leads to more and stronger interactions between the molecular entities which restrict the intramolecular motion and/or rotation of AIE luminophores and effectively prevent nonradiative relaxation mechanisms. This supports the relaxation through the emission of light and leads to fluorescence or phosphorescence.[10–13] However, LC-materials may also show properties of fluids with smaller intermolecular forces in comparison to the crystalline state, thereby supporting radiative relaxation of ACQ luminophores. In the same context the emission of AIE luminophores is decreased or quenched. This emission phenomenon led to the development of thermo-responsive emissive materials. For example, in 2021, Ke Xue *et al.* developed a fluorescent nanothermometer in the temperature range from 25 to 45 °C. They utilized a fatty acid as the host material for an AIE luminophore. By increasing the temperature, the molecular arrangement of the fatty acid was altered, yielding a change in polarity. This change in the environment of the luminophore resulted in a change of its emission properties.[14] In 2022, Wang *et al.* prepared a single component material of difluoroboron diphenyl β-diketonate, which changes its emission colour from green to blue. The temperature change influences the intermolecular forces between the molecular entities yielding excimeric or monomeric species with different emission properties.[15]

In 2018, our group started to investigate emissive liquid crystalline materials and we developed different approaches to overcome the design challenges of luminescent LCs with tuneable fluorescence properties.[10] In 2020, we utilized a supramolecular approach with hydrogen-bonded LCs. As donor units different hydroxybenzoic acids were used in combination with 4-alkoxystilbazoles as hydrogen bond acceptors. These assemblies exhibit turn-on fluorescence when irradiated with UV-light (405 nm) in the mesophase. The reason for this phenomenon is a photo-initiated proton transfer which is reversible by thermal treatment.[16] In another study dynamic covalent bonded liquid crystals were used to develop materials with tuneable fluorescence. For this study we choose salicylimines which are known to show photoluminescence caused by *e.g.* excited-state intramolecular proton transfer (ESIPT) or crystallization enhanced emission.[17,18] This led to emissive LC materials that show the characteristic AIE behaviour upon thermal treatment. The dynamic nature of the imine bonds was employed for *in situ* manipulation of the fluorescence behaviour, by making use of

[a] Organic Chemistry, University of Duisburg Essen, Universitätsstraße 7, Essen 45117, Germany
[b] Co-Creationlab Product Innovations, University of Duisburg Essen, Schützenbahn 70, Essen 45127, Germany. E-mail: michael.giese@uni-due.de

† Electronic supplementary information (ESI) available. See DOI: https://doi.org/10.1039/d5tc01954k

imine exchange reactions.[6] Recent work by us and Strassert *et al.* showed an approach using phosphorescent metallomesogens to yield luminescent liquid crystals. In this study two series of Pt(II) complexes were synthesized with different aggregation possibilities. This influences and controls the Pt–Pt coupling, which is crucial for the design of photo functional Pt(II) mesogens.[5]

Results and discussion

Since we are interested in materials with tuneable fluorescence behaviour we were curious to know how two classes of luminophores, namely ACQ and AIE luminophores, mutually effect the emissive properties. While common systems employ either an AIE or an ACQ luminophore for the introduction of fluorescence, we herein combine both classes of luminophores, in order to tune the emission behaviour of liquid crystalline materials. Thereby, we use the unique features between order and fluidity of the liquid crystalline state with the characteristic behaviour of ACQ and AIE emitters. For this we use a liquid crystalline AIE luminophore as the host which emits green light and dope the material with a red-emitting ACQ luminophore. In the crystalline state the emission of the material is dominated by the AIE luminophore while in the isotropic state the ACQ emitter controls the emission behaviour. Consequently, the fluorescence behaviour of the hybrid material will be controlled by the state of aggregation, which can be tuned by temperature. The underlying concept and the specific luminophores for the present study are depicted in Fig. 1. **Im-CN-C$_8$** (yellow, Fig. 1) and **Im-Cl-C$_8$** (green, Fig. 1) are new mesomorphic materials which are structurally related to previously reported systems of our group. They show the characteristic behaviour of an AIE emitter in THF/H_2O mixtures with varying amounts of water (ESI,† Fig. S20).[6] As an ACQ luminophore we chose the maleonitrile-based salen ***cis*-Sal** (red, Fig. 1) which is known in the literature and exhibits red emission in solution, but no emission in the solid state.[19] By balancing the composition of the system and fine-tuning of the emission and liquid crystalline behaviour, a system was created to mimic a traffic light. This mimic shows a change in fluorescence from green (not hot, can be touched) to red (hot, do not touch) upon heating to 60 °C.

The salicylimines and salen used in the present manuscript were synthesized *via* literature known procedures (see the ESI† for details).[20] Subsequently the obtained salicylimines (**Im-CN-C$_8$**, **Im-Cl-C$_8$**) and ***cis*-Sal** were investigated with respect to their mesophase and temperature-dependent fluorescence behaviour. The phase behaviour under a polarized optical microscope (POM) is summarized in Fig. 2. Upon heating **Im-CN-C$_8$** exhibits a smectic phase from 82 to 85 °C, followed by a transition into the nematic phase at 85 °C. The clearing point of the material is reached at 95 °C (see the ESI,† Fig. S7 and S9). Upon cooling from the isotropic phase liquid crystallinity is restored at 92 °C, showing a nematic texture under the POM. After transition to the smectic phase at 82 °C the mesophase remains until 57 °C where crystallization takes place (Fig. 2 and the ESI,† Fig. S7G). In contrast **Im-Cl-C$_8$** shows an enantiotropic smectic phase (Fig. 2 and the ESI,† Fig. S5B, D, S9) from 59 to 94 °C on heating and from 88 to 24 °C on cooling and therefore shows liquid crystallinity around room temperature. All transition temperatures were confirmed *via* differential scanning

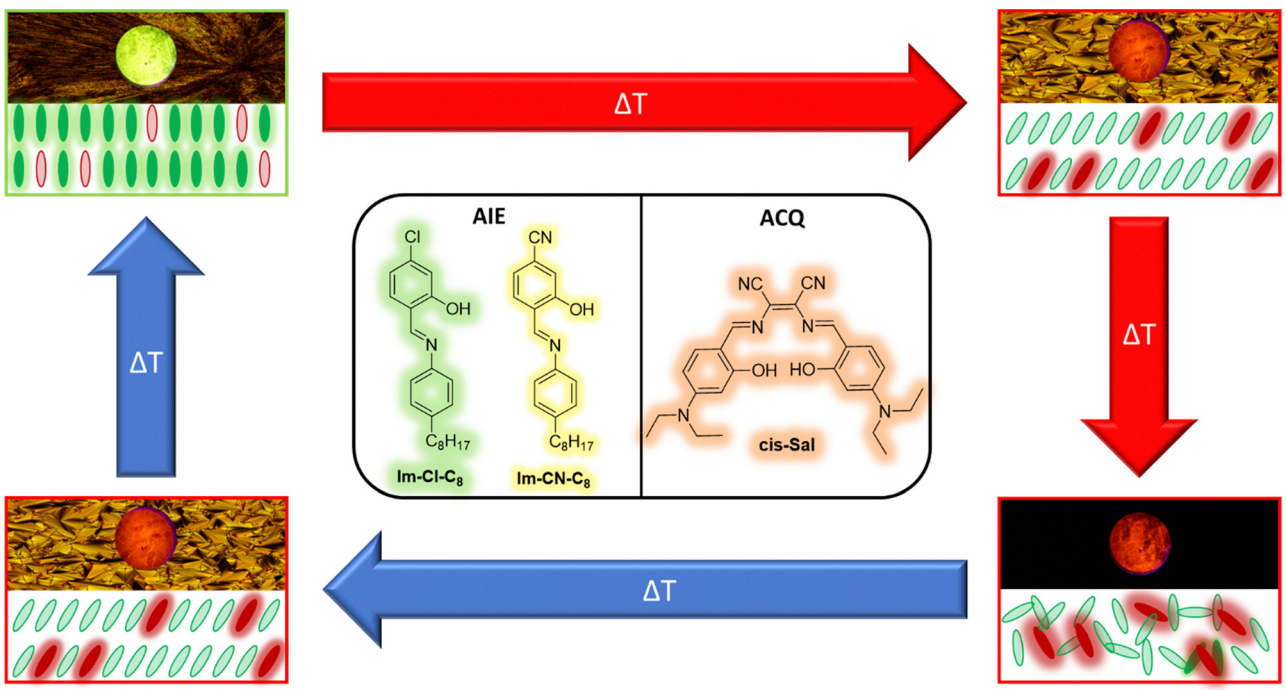

Fig. 1 Scheme of thermal fluorescence tuning due to phase transitions of the AIE host mesogens **Im-Cl-C8** (green) and **Im-CN-C$_8$** (yellow) in combination with the ACQ luminophore ***cis*-Sal** (red).

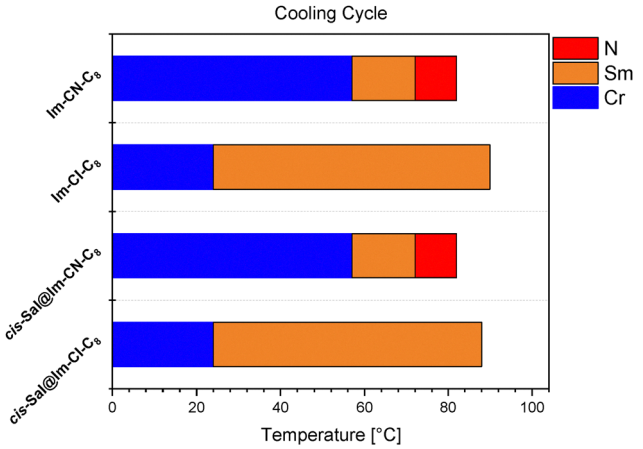

Fig. 2 Mesomorphic properties of the investigated imines and their respective host–guest materials with ***cis*-Sal**. Phase transitions and transition temperatures were obtained using a POM upon cooling at a rate of 10 °C min^{-1} (Cr: crystalline, Sm: smectic, N: nematic.).

calorimetry (DSC) (see the ESI,† Fig. S10 and S11). ***Cis*-Sal** does not show mesomorphism and decomposes at ~300 °C.

Salicylimines are known to show aggregation and crystallization dependent luminescence, which is caused by excited state intramolecular proton transfer (ESIPT), restriction of intramolecular motion/vibration or/and aggregation enhanced emission.[17,18,21,22] Therefore, a change in the emission behaviour is expected by changing the order and state of aggregation. To investigate this, variable temperature fluorescence spectroscopy was performed. To this end, the samples were heated/cooled between 30 and 110 °C and the change in emission was investigated *via* fluorescence spectroscopy. At room temperature **Im-Cl-C8** shows a green emission with a maximum at 537 nm (see Fig. 3), while **Im-CN-C_8** emits yellow/green light at 560 nm (see ESI,† Fig. S15). During the heating and cooling cycles both materials show a similar change in their emission behaviour. Upon heating **Im-Cl-C_8** exhibits a decreasing emission intensity. Up to 50 °C the emission intensity decreases slowly and drops drastically at 60 °C. This drop in emission intensity is correlated with a phase transition from the crystalline to the smectic phase (Fig. 2 and the ESI,† Fig. S5B). At 110 °C the emission intensity is almost vanished (4% of the initial intensity). Upon cooling the intensity of the emission maximum slowly increases between 110 and 40 °C. A

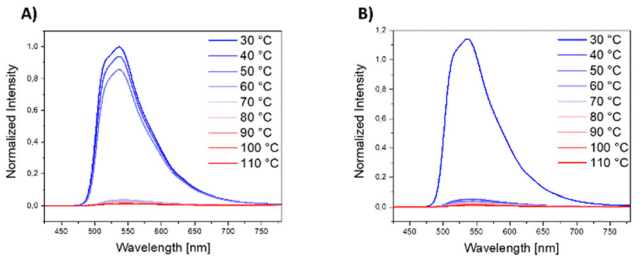

Fig. 3 Fluorescence spectra of **Im-Cl-C_8** on heating (A) and cooling (B) into the isotropic state. Excitation wavelength: 405 nm.

significant increase in the emission intensity is observable at 30 °C, which correlates with the crystallization of the material (see Fig. 2 and the ESI,† Fig. S5E). For **Im-CN-C_8** a similar behaviour was observed with drastic changes in the intensity at 90 and 60 °C upon heating/cooling (see the ESI,† Fig. S14). For further characterization of the photophysical properties of the two AIE emitters we measured photoluminescence quantum yields at room temperature in the solid state. **Im-Cl-C_8** showed a moderate quantum yield of Φ_L = 0.22 ± 0.02. **Im-CN-C_8** exhibits a similar value with a quantum yield of Φ_L = 0.23 ± 0.02. Accordingly, both salicylimines are suitable host materials for the development of the fluorescent traffic light. For the ACQ luminophore ***cis*-Sal** we did not measure temperature-dependent fluorescence data, since the compound did not show mesomorphism and decomposed at 300 °C.

In order to prepare responsive materials for thermo sensing **Im-Cl-C_8** or **Im-CN-C_8** were used as LC host materials and doped with ***cis*-Sal** (for details see the ESI†). The final mixtures ***cis*-Sal@Im-Cl-C_8** and ***cis*-Sal@Im-CN-C_8** contain 0.025 mol% of ***cis*-Sal** as the ACQ emitter. It should be noted that the mixtures did not show any exchange reactions between the components. Initially the effect of doping, on the phase sequence and transition temperatures, has been investigated by POM and DSC measurements. The mixtures ***cis*-Sal@Im-Cl-C_8** and ***cis*-Sal@Im-CN-C_8** show no significant change in the phase sequence or transition temperatures in comparison to the pristine host materials **Im-Cl-C_8** and **Im-CN-C_8** (see Fig. 2 and Fig. S5–S13, ESI†). To get a first insight into the emission properties when the ACQ luminophore is ''off'' and the ACQ luminophore is ''on'' we performed fluorescence measurements in DCM solution (see Fig. S20, ESI†). There we could observe as expected the emission signals of the AIE (~530 nm **Im-Cl-C_8** and ~550 nm **Im-CN-C_8**) and ACQ (613 nm ***cis*-Sal**) luminophores where the ACQ emitter shows a higher emission intensity. To get further insight, for two luminophores influencing the emission behaviour of one another, we investigated the possibility of Förster resonance energy transfer in the solid state. In general, FRET is evaluated by comparing the fluorescence lifetime of the donor in the absence and presence of an acceptor.[23–25] To assess the possibility of FRET in our system, time-resolved photoluminescence measurements were performed for the AIE-active luminophores **Im-Cl-C_8** and **Im-CN-C_8**, both in the presence and absence of the ***cis*-Sal**.

As shown in Fig. 4A, the fluorescence lifetime of **Im-Cl-C_8** remains effectively unchanged in the presence of ***cis*-Sal**. The measured lifetime of **Im-Cl-C_8** in the ***cis*-Sal@Im-Cl-C_8** was 2.61 ± 0.01 ns, which is nearly identical to that of **Im-Cl-C_8** in the absence of ***cis*-Sal** (2.62 ± 0.09 ns, see the ESI,† Fig. S21 and 22). A similar trend was observed for **Im-CN-C_8** (see Fig. 4B), where no significant change in fluorescence lifetime was detected upon addition of ***cis*-Sal** (see the ESI,† Fig. S23 and S24). These results indicate that the presence of ***cis*-Sal** does not alter the fluorescence lifetimes of **Im-Cl-C_8** and **Im-CN-C_8**. Therefore, we conclude that FRET between the AIE luminophores and ***cis*-Sal** is negligible under the investigated conditions.

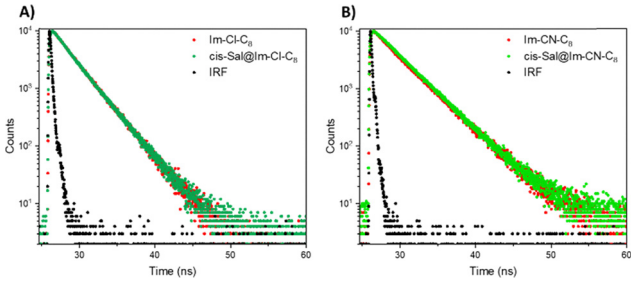

Fig. 4 Time-resolved fluorescence decay curves of (A) **Im-Cl-C$_8$** and ***cis*-Sal@Im-Cl-C$_8$**; (B) **Im-CN-C$_8$** and ***cis*-Sal@Im-CN-C$_8$**. As the fluorescence lifetime is shorter, the instrument response function (IRF) was measured to minimize errors *via* deconvolution.

To prove the tuning of the emissive behaviour by phase transition, the mixtures of AIE and ACQ luminophores ***cis*-Sal@Im-Cl-C$_8$** and ***cis*-Sal@Im-CN-C$_8$** were investigated *via* variable temperature fluorescence spectroscopy. In addition to that photographs were taken during heating and cooling under UV-light (see Fig. 5 and the ESI,† Fig. S18). The fluorescence spectrum of ***cis*-Sal@Im-Cl-C$_8$** at 30 °C shows two emission maxima, one at 534 nm and one with a lower relative intensity at 639 nm (see Fig. 5B). The maximum at 534 nm can be correlated to **Im-Cl-C$_8$** while the maximum at 639 nm is caused by the ACQ luminophore ***cis*-Sal**. An emission signal of the ACQ luminophore in the crystalline state could be caused by weaker interactions in the mixture than in the pure crystal of ***cis*-Sal** which counteracts full quenching of the fluorescence.[26–28] Photographs under UV-light at 30 °C clearly show a green emission visible by the naked eye (see Fig. 4A). Upon heating the emission maximum at 534 nm slowly decreases, while the maximum at 639 nm exhibits no significant change. At 60 °C the liquid crystalline host passes into the smectic phase which is correlated with a drastic change in emission intensity of the signal at 534 nm. This is accompanied by an increase of the emission intensity and a hypsochromic shift to 619 nm of the signal at 639 nm (see Fig. 5B). Both luminophores show the expected change in emission intensity by entering the LC phase and the related change in aggregation and order. This leads to a bathochromic shift of the global emission maxima from 539 nm to 619 nm which is also visible to the naked eye (see Fig. 5A). With the crystallization process starting at 30 °C a hypsochromic shift of the global emission maximum to 534 nm is observed. The wavelength of the maximum in the red region of the visible spectrum shifts back to 639 nm and recovers its initial emission intensity (see Fig. 5C). The emission returns to its initial green colour as proven by photographs (see Fig. 5A). In order to prove that the temperature-dependent change in the fluorescence is reversible five heating/cooling cycles were performed, showing no significant changes of the starting and final emission behaviour (see Fig. S17, ESI†). These results show that the combination of different types of luminophores in a liquid crystalline material provide access to luminescent materials with thermal response. The obtained emission spectra indicate that in the mixture of ***cis*-Sal@Im-Cl-C$_8$** both luminophores seem to act independently and do not interfere with each other. The global emission behaviour

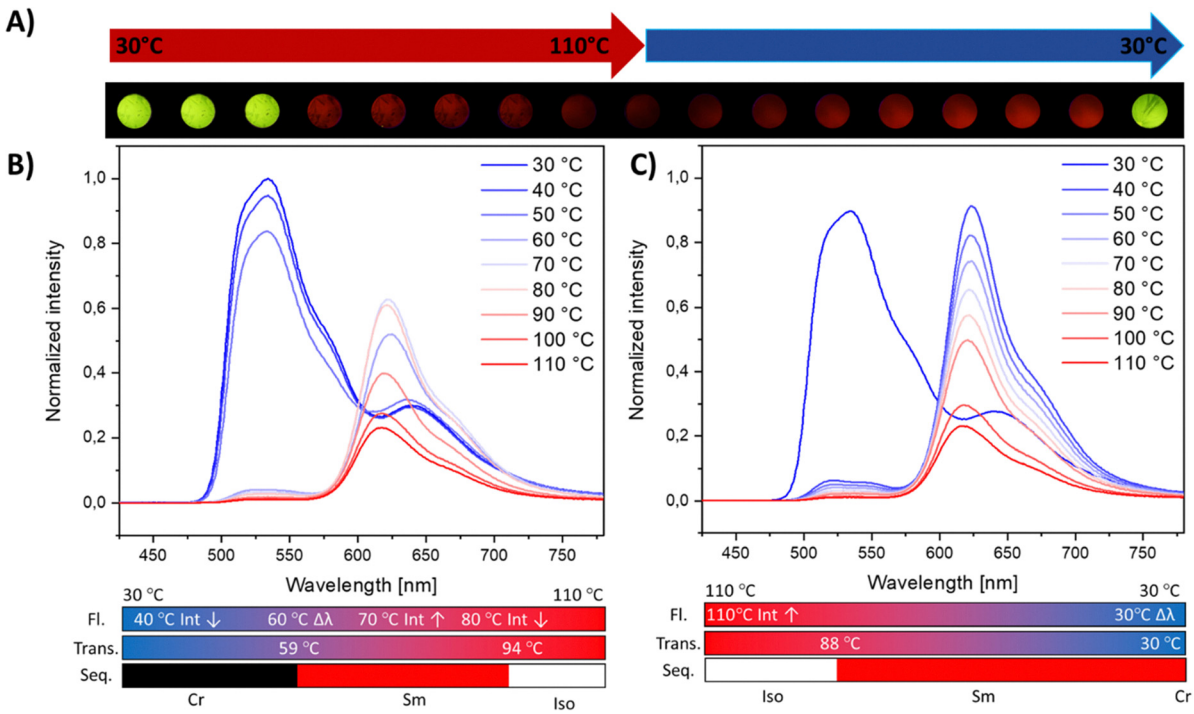

Fig. 5 Photographs (A) and fluorescence spectra of ***cis*-Sal@Im-Cl-C$_8$** on heating (B) and cooling (C) into the isotropic state. Excitation wavelength: 405 nm.

is dominated by the AIE or the ACQ emitter, yielding a red emission at higher temperatures and a green emission at lower temperatures. In order to prove that this approach can be transferred to related systems, we produced the ***cis*-Sal@Im-CN-C_8** mixture. At 30 °C the ***cis*-Sal@Im-CN-C_8** mixture shows two distinct emission maxima one at 545 nm which correlates with the AIE luminophore **Im-CN-C_8** and the second at 628 nm corresponding to the ACQ dopant (see the ESI,† Fig. S18). In comparison to the ***cis*-Sal@Im-Cl-C_8** system the ***cis*-Sal@Im-CN-C_8** mixture shows a relatively stronger emission intensity at 628 nm with a hypsochromic shift of 11 nm. A possible explanation is that the ACQ luminophore is incorporated in the host material with weak intermolecular interactions which enhance the fluorescence in comparison to the quenching of strong π–π interactions (see Fig. S18B, ESI†).[27,29] With the naked eye an overlay of both luminophores is observed yielding a yellow/orange emission (see Fig. S18A, ESI†). Upon heating, initially both local maxima decrease slightly in emission intensity (see Fig. S18B, ESI†). This could be associated with the increased nonradiative relaxation of the excited electrons due to more intramolecular motion, internal conversion or similar processes.[30] At around 80 °C the sample passes into the LC-phase, with the lower order yielding a strong decrease of the emission signal of the AIE luminophore at 545 nm. In contrast, the global maximum at 628 nm, which can be associated with the ACQ luminophore ***cis*-Sal**, undergoes a bathochromic shift and increase in the emission intensity. This is attributed to weaker interactions in the LC-phase facilitating radiative relaxation of ***cis*-Sal**. For the naked eye this leads to a colour change of the visible emission from yellow/orange to red (see Fig. S18A, ESI†). Upon further heating to 110 °C the material exhibits an overall decrease of emission intensity. For the cooling cycle the process is reversed (see Fig. S18C, ESI†) showing an increase of both emission signals in the temperature range from 110 to 60 °C. At the start of the crystallization process below 60 °C the fluorescence spectra of ***cis*-Sal@Im-CN-C_8** exhibits a hypsochromic shift of the global emission maxima and both maxima return to their initial emission intensity, leading to the change of the visible emission colour from red to yellow/orange at 50 °C and below. The whole process of tuning the emission colour of the material ***cis*-Sal@Im-CN-C_8** from yellow/orange to red is reversible for at least 5 heating/cooling cycles. To test the thermosensing potential of the material we created a dual sensor array of thin films of ***cis*-Sal@Im-Cl-C_8** (left) and ***cis*-Sal@Im-CN-C_8** (right) on a glass slide. The glass slide was placed on a metal block and the right part of the metal block was heated to create a temperature gradient (see Fig. 6). Initially, at room temperature, the sensor shows green and yellow fluorescence displaying that the sample is cold and can be touched (see Fig. 6A). After a few minutes of heating red emission propagates through the green material showing that the sample undergoes a phase transition at an elevated temperature (see Fig. 6B). After a few seconds the green emission is fully vanished and the left part of the sensor appears red emissive, while the right part of the

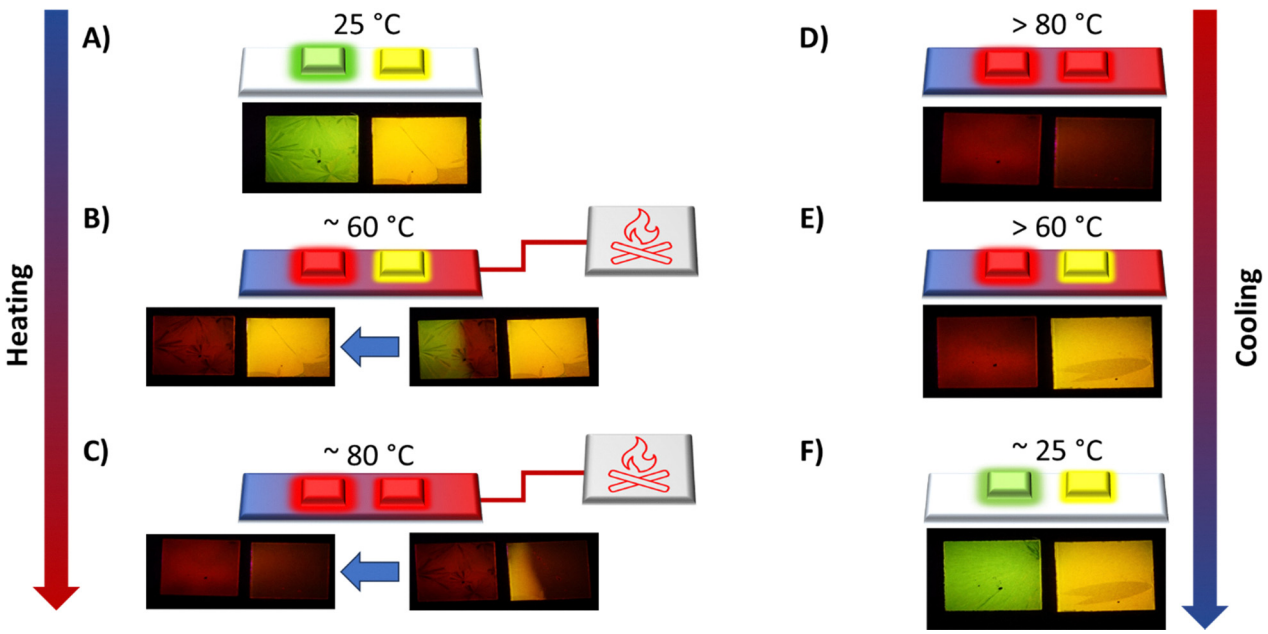

Fig. 6 Schematic representation of the thermosensor of ***cis*-Sal@Im-Cl-C_8** and ***cis*-Sal@Im-CN-C_8** on a glass slide (upper image) as well as photographs of the fluorescent sample (lower images). (A) Sensor materials without heating showing green/yellow emission (room temperature). (B) Sensor materials after connecting the glass slide with a heat source from the right showing red/yellow emission (temperature ~ 60 °C). (C) Sensor materials after further heating time showing red/red emission (temperature ~80 °C). (D) Sensor materials after disconnecting the glass slide from the heating source showing red/red emission (temperature >80 °C). (E) Sensor materials after cooling showing red/yellow emission (temperature >60 °C). (F) Sensor materials after further cooling time showing green/yellow emission (temperature ~25 °C).

sensor shows yellow emission. This represents a temperature of around 60 °C (see Fig. 6B) and asks for caution when touching the material. At temperatures above 80 °C both parts of the sensor appear red, providing a heat warning (see Fig. 6C). After removing the heat source, the right part of the sensor switches back to a yellow fluorescence between 80 and 60 °C (see Fig. 6E). Further cooling restores the initial green/yellow emission state at temperatures below 60 °C (see Fig. 6F).

Conclusions

In conclusion, we reported a new approach towards thermosensing based on luminescent materials. By combining two types of luminophores in a liquid crystalline environment we were able to mimick a traffic light for heat warning. The mixture of an AIE and ACQ emitter combined with the temperature-dependent order of the liquid crystalline state allowed tuning of the fluorescence colour from green (534 nm) at lower temperature to red (639 nm) at higher temperatures (for the ***cis*-Sal@Im-Cl-C8** system). The shift of the emission wavelength by 105 nm was possible due to the temperature-controlled adjustment of the intermolecular interactions in the different phases. The emission behaviour of AIE and ACQ emitters strongly depend on the local environment and the interactions between the emitter and the molecular environment. Therefore, a temperature induced change in the local surrounding of the luminophores allows tuning of the emission behaviour, while the luminescence behaviour at room temperature is dominated by the emission of the AIE luminophore in the highly ordered and confined environment of the crystalline state. The red emission at elevated temperatures is dictated by the ACQ emitter. The liquid crystalline and isotropic phase exhibit weakened intermolecular interactions in the local environment, allowing radiative relaxation. This first proof-of-concept indicates that the combination of different types of luminophores in a liquid crystalline matrix provides a promising route for the development of thermoresponsive materials with tuneable emission. Further activities in our group will focus on the transfer and generalization of this approach to other luminophores and liquid crystalline materials.

Author contributions

The manuscript was written through contributions of all authors. All authors have given approval to the final version of the manuscript.

Conflicts of interest

The authors declare no conflict of interests.

Data availability

The data supporting this article have been included as part of the ESI.†

Acknowledgements

M. G. thanks the DFG for generous financial support (Heisenberg Program, 443479537).

Notes and references

1 X. Hao, B. Xiong, M. Ni, B. Tang, Y. Ma, H. Peng, X. Zhou, I. I. Smalyukh and X. Xie, *ACS Appl. Mater. Interfaces*, 2020, **12**, 53058–53066.
2 M. Mitani, M. Yoshio and T. Kato, *J. Mater. Chem. C*, 2017, **5**, 9972–9978.
3 R. K. Gupta, D. Das, M. Gupta, S. K. Pal, P. K. Iyer and A. S. Achalkumar, *J. Mater. Chem. C*, 2017, **5**, 1767–1781.
4 Y. Wang, J. Shi, J. Chen, W. Zhu and E. Baranoff, *J. Mater. Chem. C*, 2015, **3**, 7993–8005.
5 M. E. Gutierrez Suburu, M. Blanke, L. Geerkens, A. Hepp, I. Maisuls, J. Kösters, T. Neumann, J. Voskuhl, M. Giese and C. A. Strassert, *Aggregate*, 2024, **5**, e473.
6 M. Blanke, T. Neumann, M. E. Gutierrez Suburu, O. Prymak, C. Wölper, C. A. Strassert and M. Giese, *ACS Appl. Mater. Interfaces*, 2022, **14**, 55864–55872.
7 S. Jiang, J. Qiu, Y. Chen, H. Guo and F. Yang, *Dyes Pigm.*, 2018, **159**, 533–541.
8 M. Mitani, M. Yoshio and T. Kato, *J. Mater. Chem. C*, 2017, **5**, 9972–9978.
9 H. Lu, S. Zhang, A. Ding, M. Yuan, G. Zhang, W. Xu, G. Zhang, X. Wang, L. Qiu and J. Yang, *New J. Chem.*, 2014, **38**, 3429–3433.
10 J. Voskuhl and M. Giese, *Aggregate*, 2022, **3**, e124.
11 Y. Wang, J. Shi, J. Chen, W. Zhu and E. Baranoff, *J. Mater. Chem. C*, 2015, **3**, 7993–8005.
12 Z. He, C. Ke and B. Z. Tang, *ACS Omega*, 2018, **3**, 3267–3277.
13 J. Mei, N. L. C. Leung, R. T. K. Kwok, J. W. Y. Lam and B. Z. Tang, *Chem. Rev.*, 2015, **115**, 11718–11940.
14 K. Xue, C. Wang, J. Wang, S. Lv, B. Hao, C. Zhu and B. Z. Tang, *J. Am. Chem. Soc.*, 2021, **143**, 14147–14157.
15 J.-X. Wang, L.-Y. Peng, Z.-F. Liu, X. Zhu, L.-Y. Niu, G. Cui and Q.-Z. Yang, *J. Phys. Chem. Lett.*, 2022, **13**, 1985–1990.
16 A. Kappelt and M. Giese, *Chem. – Eur. J.*, 2020, **26**, 13347–13351.
17 Y. Dong, J. W. Y. Lam, A. Qin, Z. Li, J. Sun, Y. Dong and B. Z. Tang, *J. Inorg. Organomet. Polym. Mater.*, 2007, **17**, 673–678.
18 A. C. Sedgwick, L. Wu, H.-H. Han, S. D. Bull, X.-P. He, T. D. James, J. L. Sessler, B. Z. Tang, H. Tian and J. Yoon, *Chem. Soc. Rev.*, 2018, **47**, 8842–8880.
19 X. Ma, R. Sun, J. Cheng, J. Liu, F. Gou, H. Xiang and X. Zhou, *J. Chem. Educ.*, 2016, **93**, 345–350.
20 H. Xu, Z. Huang, Y. Li, B. Gu, Z. Zhou, R. Xie, X. Pang, H. Li and Y. Zhang, *Analyst*, 2018, **143**, 4354–4358.
21 J. Mei, N. L. C. Leung, R. T. K. Kwok, J. W. Y. Lam and B. Z. Tang, *Chem. Rev.*, 2015, **115**, 11718–11940.
22 J. C. Germino, C. A. Barboza, F. J. Quites, P. A. M. Vazquez and T. D. Z. Atvars, *J. Phys. Chem. C*, 2015, **119**, 27666–27675.
23 C. Li, Q. Liu and S. Tao, *Nat. Commun.*, 2022, **13**, 6034.
24 C. Fang, Y. Huang and Y. Zhao, *Am. J. Transl. Res.*, 2023, **15**, 694–709.

25 H. Wang, X. Pan, W. Liu, Y. Huang, X. Yi and Z. Chen, *Chem. Eng. J.*, 2024, **486**, 150432.
26 T. M. Figueira-Duarte, P. G. Del Rosso, R. Trattnig, S. Sax, E. J. W. List and K. Müllen, *Adv. Mater.*, 2010, **22**, 990–993.
27 S. Dai, Y. Zhou, H. Zhang, Z. Cai, B. Tong, J. Shi and Y. Dong, *J. Mater. Chem. C*, 2020, **8**, 11177–11184.
28 Y. Liu, Y. Lv, X. Zhang, S. Chen, J. W. Y. Lam, P. Lu, R. T. K. Kwok, H. S. Kwok, X. Tao and B. Z. Tang, *Chem. – Asian J.*, 2012, **7**, 2424–2428.
29 T. M. Figueira-Duarte, P. G. Del Rosso, R. Trattnig, S. Sax, E. J. W. List and K. Müllen, *Adv. Mater.*, 2010, **22**, 990–993.
30 S. M. Hanagodimath, B. Siddlingeshwar, J. Thipperudrappa and S. K. B. Hadimani, *J. Lumin.*, 2009, **129**, 335–339.